

Supplemental material

Supplemental Figures

- S1** Cell composition of the TIME in OSCC (STA).
- S2** Overview of all cell masks colored by cell type (UOP).
- S3** Overview of all cell masks colored by cell type (STA).
- S4** Cell densities across samples and tissue zones (UOP).
- S5** Cell densities across samples and tissue zones (STA).
- S6** Inpatient test-retest reliability between ROIs of one individual patient per cell type.
- S7** Inpatient and interpatient variability of cell population densities comparing UOP and STA.
- S8** Flowchart of cross-validation and bootstrapping procedure.
- S9** Univariate comparative analysis of model features between higher and lower grade (UOP).
- S10** Univariate comparative analysis of model features between higher and lower grade (STA).
- S11** Subset analysis of model features between well, moderately, and poorly differentiated tumors (STA).

Supplemental Tables

- S1** Antibody panel.
- S2** Cohort characteristics for UOP and STA cohort.
- S3** Adjuvant treatment and patient outcomes in the STA cohort.

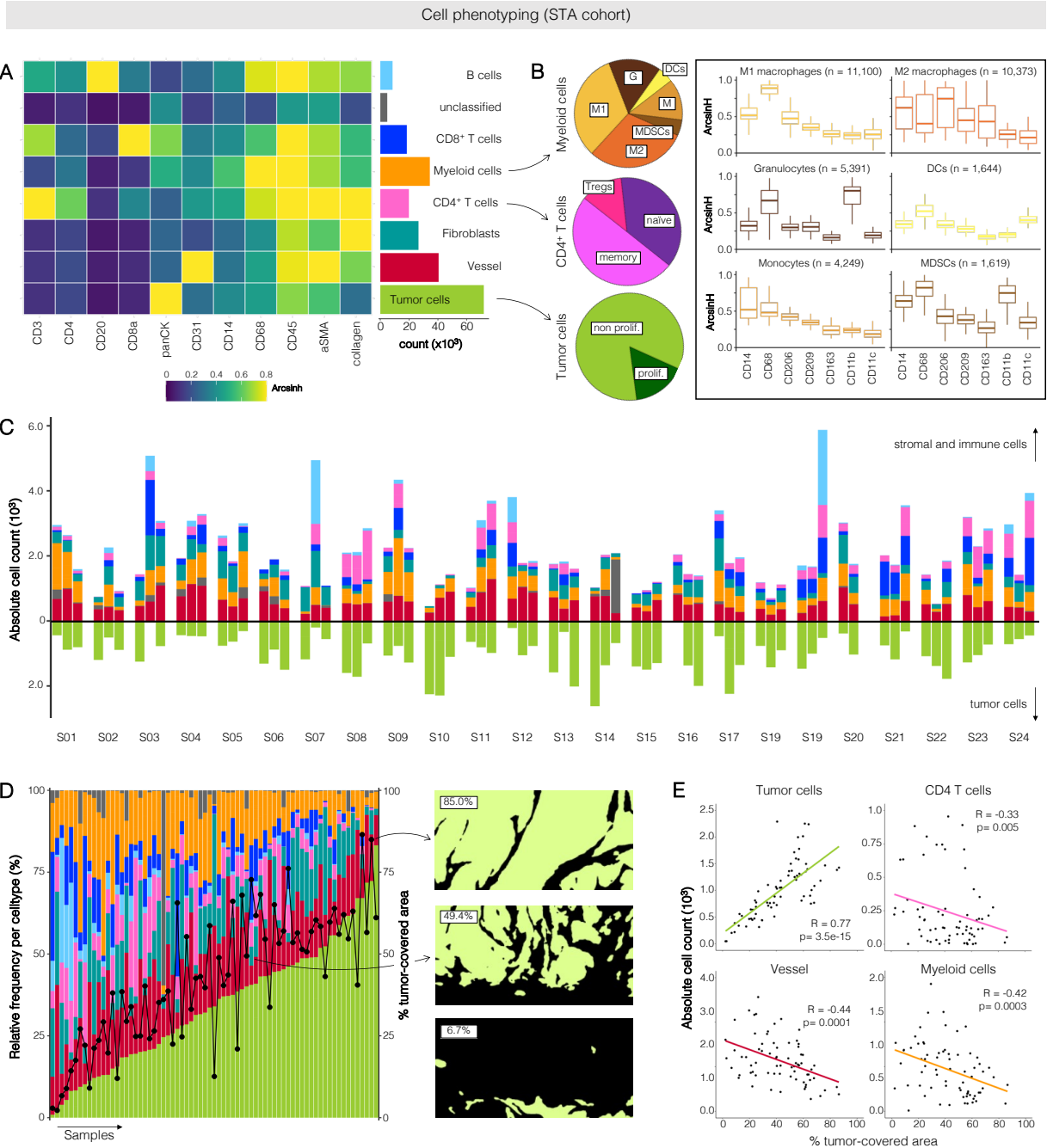


Figure S1. Cell composition of the TIME in OSCC (STA). **A** Heatmap of mean marker expression levels and absolute count of major cell subsets. **B** Relative distribution of myeloid (top left), CD4⁺ T cell (middle left), and tumor cell (bottom left) subpopulations. Marker expression levels of the respective myeloid subpopulations (right). Boxplots depict median and IQR. **C** Inter- and inpatient variability in cell abundance across ROIs. Absolute cell counts per main cell subset are depicted. **D** Relative frequency (cell count per total cell count) per main cell subset for all samples ordered by increasing tumor cell frequency (left). Black dots represent the proportion of tumor-covered area per ROI. Examples of tumor masks varying in tumor-covered area (right panels). **E** Spearman correlation between absolute cell count and the proportion of tumor-covered area per sample.



Figure S2. Overview of all cell masks colored by cell type (UOP). Main cell types (tumor cells, vessel, fibroblasts, CD4 T cells, CD8 T cells, B cells, myeloid cells, other) are depicted.



Figure S3. Overview of all cell masks colored by cell type (STA). Main cell types (tumor cells, vessel, fibroblasts, CD4 T cells, CD8 T cells, B cells, myeloid cells, other) are depicted.

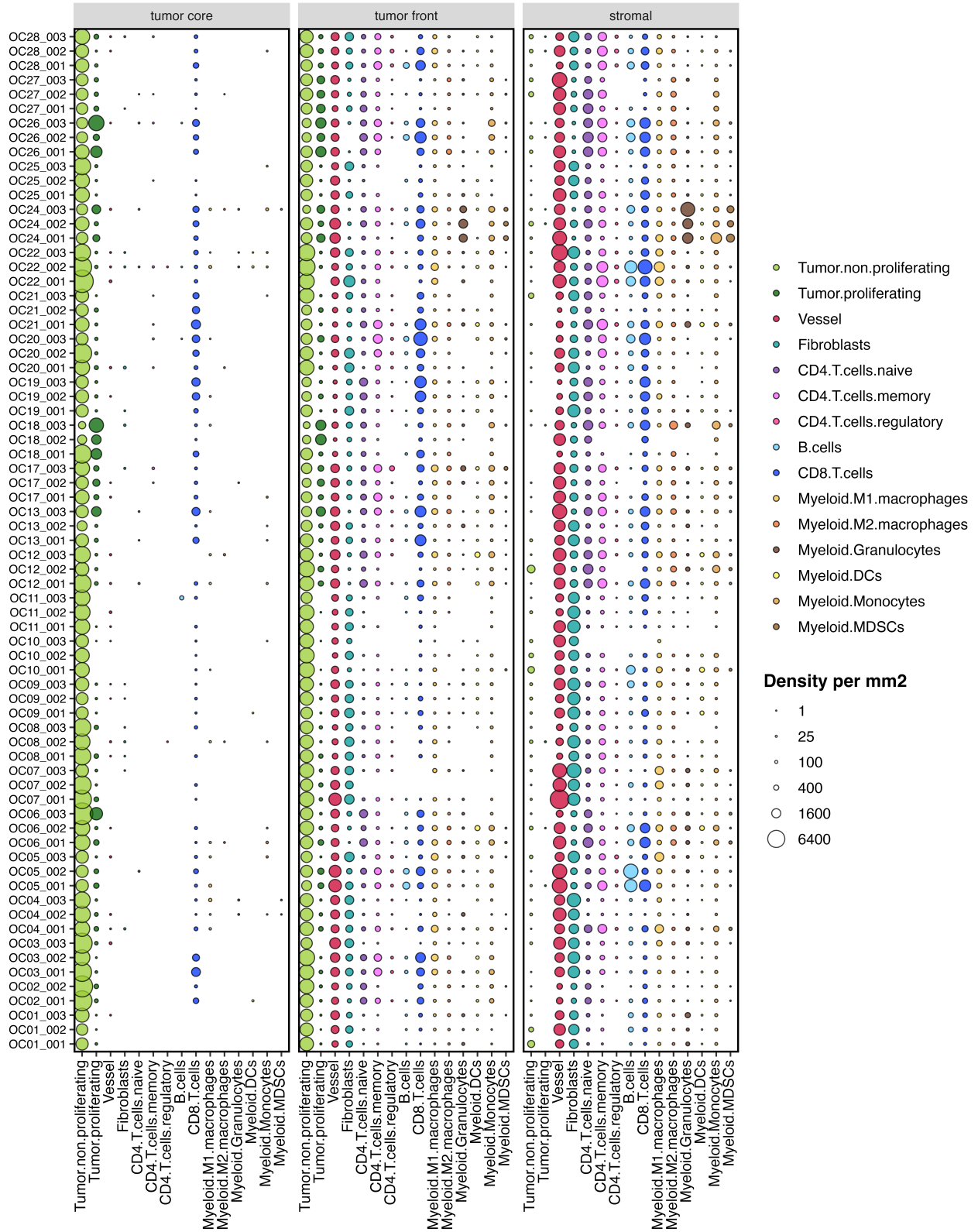


Figure S4. Cell densities across samples and tissue zones (UOP). Node size indicates the zonal cell density after subsetting (tumor core, tumor front, stromal) for all 15 identified cell subpopulations across all samples.

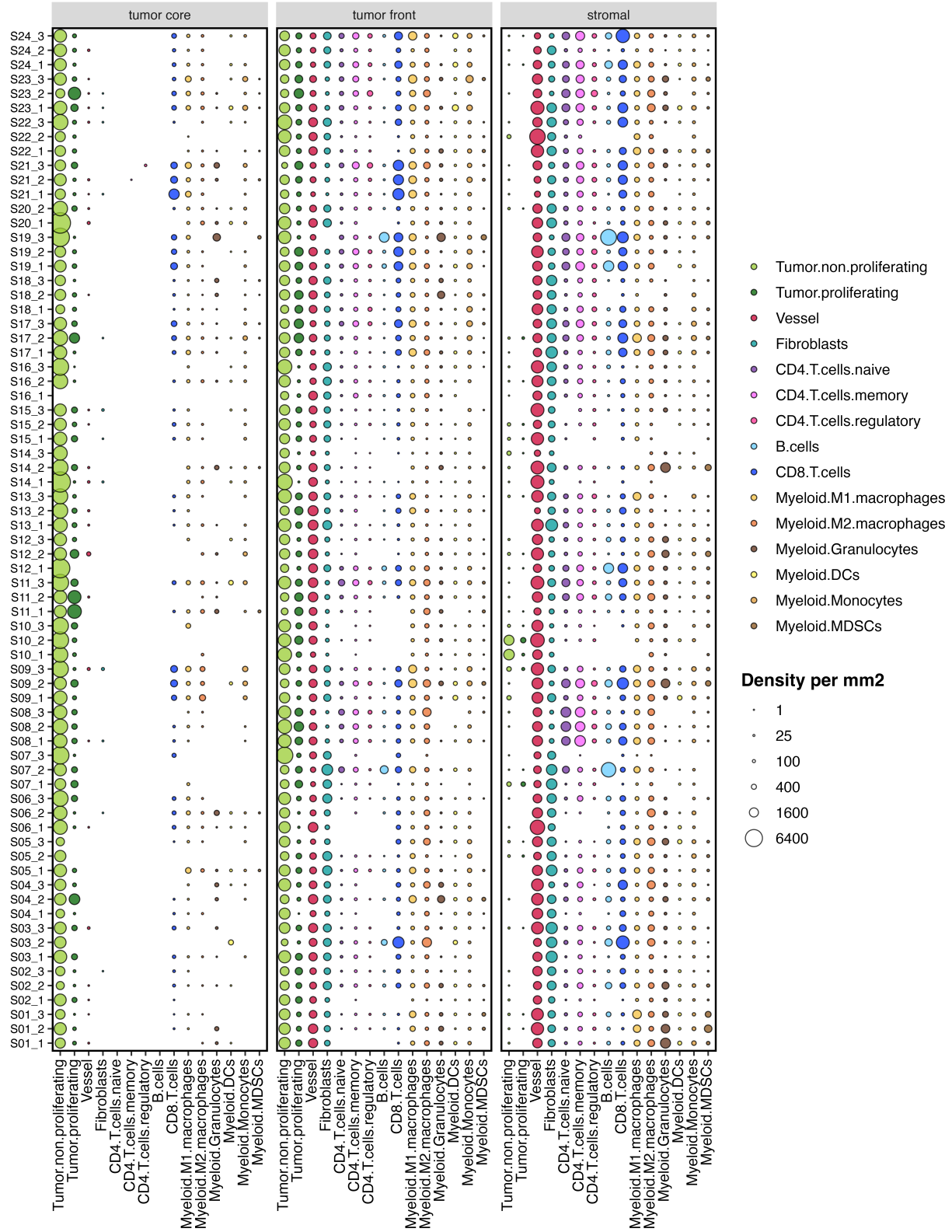


Figure S5. Cell densities across samples and tissue zones (STA). Node size indicates the zonal cell density after subsetting (tumor core, tumor front, stromal) for all 15 identified cell subpopulations across all samples.

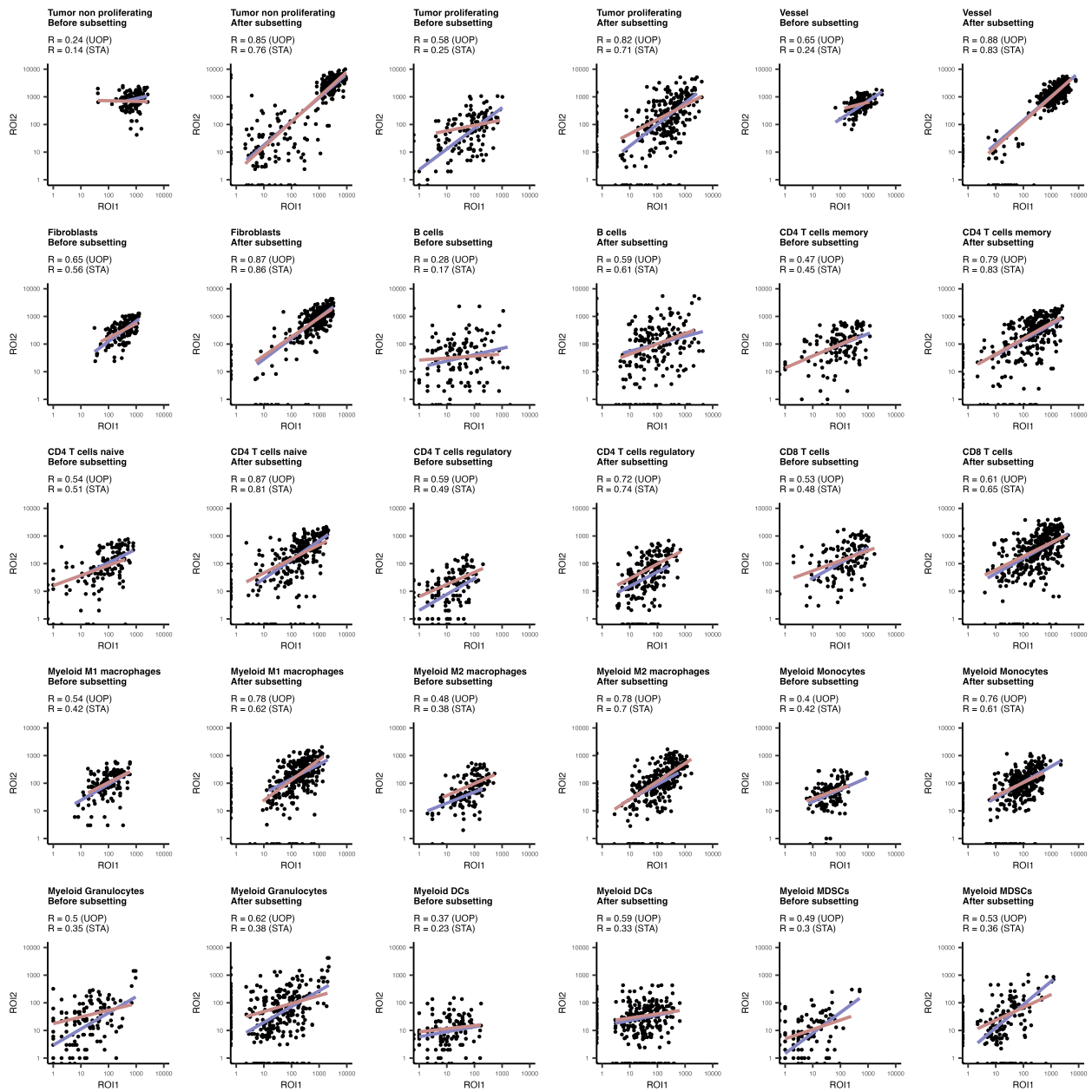


Figure S6. Inpatient reproducibility between ROIs of the same patient per cell type before and after spatial subsetting. Pairwise comparison of agreement between ROIs of the same patient for quantification of each cell type. Before spatial subsetting, the absolute count per cell population is compared between all possible pairwise combinations of two ROIs for each individual patient. After spatial subsetting, the cell population density per cell population is compared between all possible pairwise combinations of two ROIs for each individual patient. Correlation is reported for both cohorts separately (UOP: blue, STA: maroon) and was calculated using a Spearman correlation.

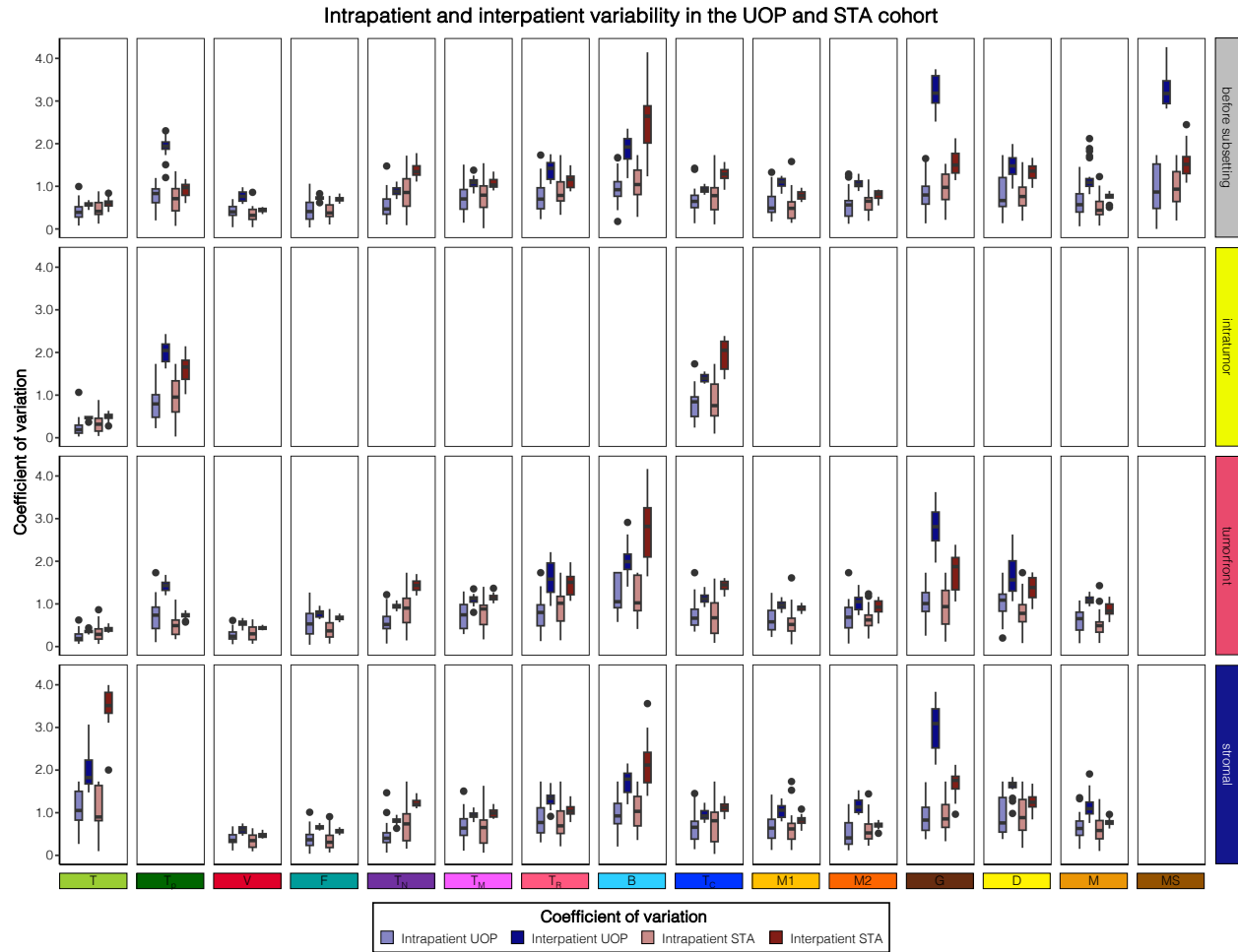


Figure S7. Inpatient and interpatient variability of cell population densities comparing UOP and STA. Inpatient and interpatient coefficients of variation (CVs) of all cell population densities before and after spatial subsetting in the two cohorts (UOP: blue, STA: maroon). CVs after spatial subsetting were only calculated for cell populations with a non-zero absolute median. For inpatient CVs, boxplots depict medians and IQR of 24 inpatient CVs calculated for each patient independently. For interpatient CVs, boxplots depict medians and IQR of 24 bootstrap iterations randomly sampling one image per patient.

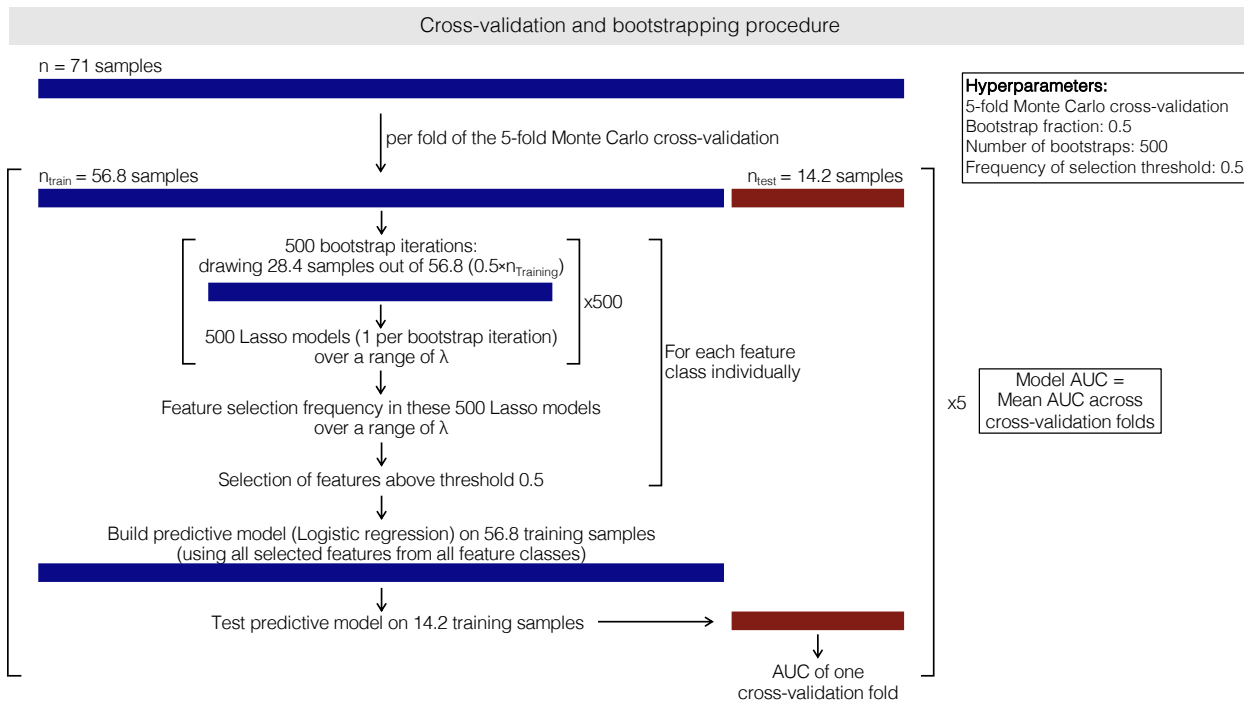


Figure S8. Model cross-validation and bootstrapping procedure. Flowchart depicting the employed cross-validation and bootstrapping procedure.

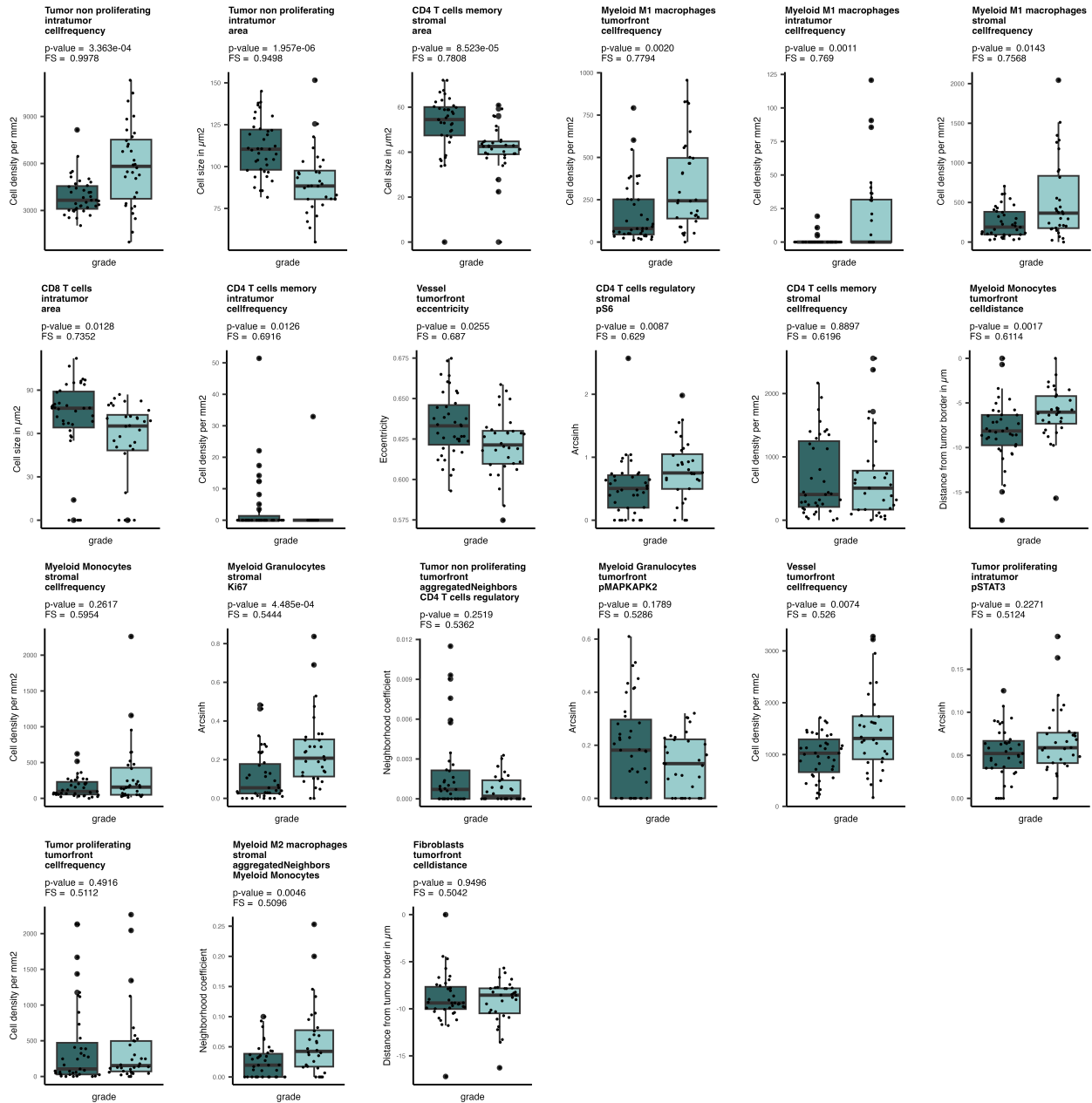


Figure S9. Univariate comparative analysis of model features between higher and lower grade (UOP). Significance between grades (lower grade: dark turquoise, higher grade: light turquoise) was calculated using a Mann Whitney U-test. Features are ordered in descending order of frequency of selection (FS) across all bootstrap model iterations. Boxplots depict medians and IQR.

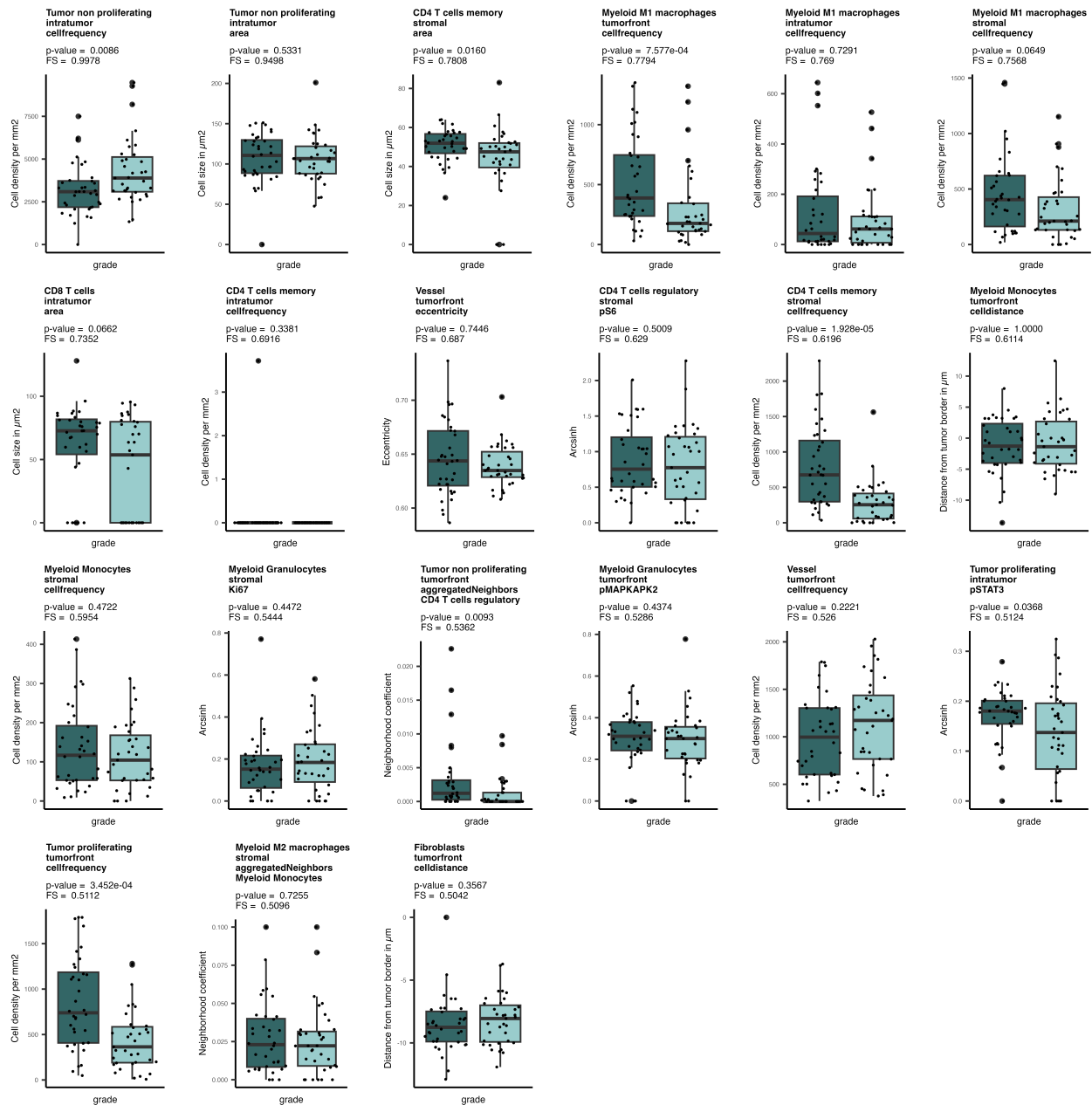


Figure S10. Univariate comparative analysis of model features between higher and lower grade (STA). Significance between grades (lower grade: dark turquoise, higher grade: light turquoise) was calculated using a Mann Whitney U-test. Features are ordered in descending order of frequency of selection (FS) across all bootstrap model iterations. Boxplots depict medians and IQR.

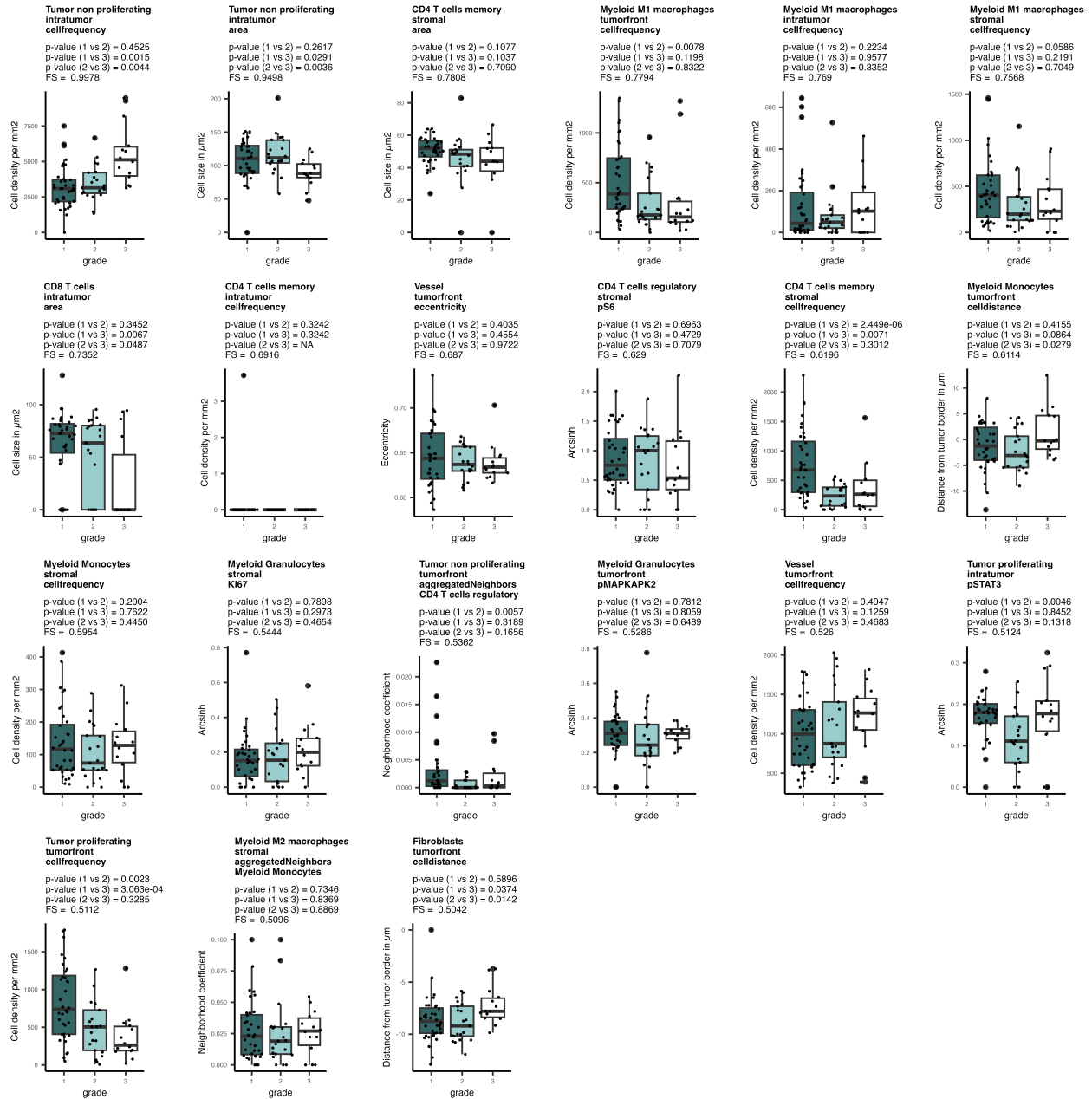


Figure S11. Subset analysis of model features between well, moderately, and poorly differentiated tumors (STA). Significance between grades well (grade 1), moderately (grade 2), and poorly (grade 3) differentiated tumors was calculated using a Mann Whitney U-test. Features are ordered in descending order of frequency of selection (FS) across all bootstrap model iterations. Boxplots depict medians and IQR.

| Metal Tag | Target | Antibody Clone | Vendor | Dilution | c (µg/ml) | Segmentation | Coarse | Fine | UOP | STA |
|-----------|------------|----------------|---------------|----------|-----------|--------------|--------|---------------|-----|-----|
| In115 | Podoplanin | D2-40 | Biolegend | 100 | 5 | membrane | | | x | |
| In115 | CD15 | W6D3 | Fluidigm | 100 | 5 | | | | | x |
| Ce140 | Vimentin | D21H3 | CST | 200 | 2.5 | membrane | yes | | x | x |
| Pr141 | aSMA | 1A4 | Invitrogen | 100 | 5 | membrane | yes | | x | x |
| Nd142 | CD206 | E2L9N | CST | 50 | 10 | membrane | | Myeloid cells | x | x |
| Nd143 | CD45RA | H1100 | Biolegend | 200 | 2.5 | membrane | | CD4 T cells | x | x |
| Nd144 | CD14 | EPR3653 | Abcam | 300 | 1.67 | membrane | yes | | x | x |
| Nd145 | CD209 | DCN46 | BD Bioscience | 50 | 10 | membrane | | Myeloid cells | x | x |
| Nd146 | CD16 | EPR16784 | Abcam | 200 | 2.5 | membrane | | | x | x |
| Sm147 | CD163 | EDHu-1 | Fluidigm | 100 | 5 | membrane | | Myeloid cells | x | x |
| Nd148 | PanCK | AE1/AE3 | Biolegend | 200 | 2.5 | membrane | yes | | x | x |
| Sm149 | CD11b | EP1345Y | Abcam | 100 | 5 | membrane | | Myeloid cells | x | x |
| Nd150 | CD86 | 37711 | Invitrogen | 100 | 5 | membrane | | | x | |
| Nd150 | HLADR | EPR3692 | Abcam | 100 | 5 | membrane | | | | x |
| Eu151 | pp38 | 36/p38 | BD Bioscience | 50 | 10 | | | | x | x |
| Sm152 | CD45 | D9M8I | CST | 200 | 2.5 | membrane | yes | | x | x |
| Eu153 | pSTAT1 | 14/p-STAT1 | BD Bioscience | 50 | 10 | | | | x | x |
| Sm154 | pSTAT3 | M9C6 | CST | 50 | 10 | | | | x | x |
| Gd155 | FOXP3 | 236A/E7 | Abcam | 100 | 5 | | | CD4 T cells | x | x |
| Gd156 | CD4 | EPR6855 | Abcam | 100 | 5 | membrane | yes | | x | x |
| Gd157 | CD36 | D8L9T | CST | 100 | 5 | membrane | | | x | x |
| Gd158 | E-Cadherin | 24E10 | CST | 100 | 5 | membrane | | | x | x |
| Tb159 | CD68 | KP1 | Biolegend | 200 | 2.5 | membrane | yes | Myeloid cells | x | x |
| Gd160 | CD31 | EP3095 | Abcam | 200 | 2.5 | membrane | yes | | x | x |
| Dy161 | CD20 | H1 | Fluidigm | 100 | 5 | membrane | yes | | x | x |
| Dy162 | CD8a | C8/144B | Biolegend | 100 | 5 | membrane | yes | | x | x |
| Dy163 | VEGF | G153-694 | Fluidigm | 200 | 2.5 | | | | x | x |
| Dy164 | CD3 | D7A6E | CST | 100 | 5 | membrane | yes | | x | x |
| Ho165 | pCREB | 87G3 | CST | 100 | 5 | | | | x | x |
| Er166 | pNFKB | EPR17622 | BD Bioscience | 100 | 5 | | | | x | x |
| Er167 | Granzyme B | EPR20129-217 | Fluidigm | 100 | 5 | | | | x | x |
| Er168 | Ki67 | B56 | Fluidigm | 100 | 5 | | | Tumor | x | x |
| Tm169 | Collagen | Polyclonal | Fluidigm | 200 | 2.5 | | yes | | x | x |
| Er170 | CD44 | IM-7 | Biolegend | 100 | 5 | membrane | | | x | x |
| Yb171 | pERK1/2 | D13.14.4E | CST | 100 | 5 | | | | x | x |
| Yb172 | CD11c | EP1347Y | Abcam | 100 | 5 | membrane | | Myeloid cells | x | x |
| Yb173 | CD56 | EPR2566 | Abcam | 300 | 1.67 | membrane | | | x | x |
| Yb174 | pMAPKAPK2 | 27B7 | CST | 100 | 5 | | | | x | x |
| Lu175 | pS6 | N7-548 | CST | 100 | 5 | | | | x | x |
| Yb176 | Histone H3 | D1H2 | Fluidigm | 300 | 1.67 | nuclear | | | x | x |
| Ir191 | DNA | Iridium | Fluidigm | 1000 | 0.5 | nuclear | | | x | x |
| Ir193 | DNA | Iridium | Fluidigm | 1000 | 0.5 | nuclear | | | x | x |

Table S1. Antibody panel. Columns coarse and fine indicate whether markers were used for RPhenograph clustering of main cell types (coarse) or subpopulations (fine). c = concentration.

| | | Full Cohort | Well differentiated | Moderately differentiated | Poorly differentiated |
|------------------------|------------------|--------------------|---------------------|---------------------------|-----------------------|
| UOP Cohort | | n = 24 | n = 13 | n = 10 | n = 1 |
| Sex | Female | 11 (46%) | 7 (54%) | 4 (40%) | 0 |
| | Male | 13 (54%) | 6 (46%) | 6 (60%) | 1 (100%) |
| Age | Mean (\pm SD) | 60.6 (\pm 16.7) | 60.6 (\pm 18.4) | 58.7(\pm 14.4) | 45 |
| | Range | 24 – 85 | 24 – 85 | 41 – 83 | – |
| Race | Caucasian | 13 (54%) | 7 (54%) | 5 (50%) | 1 (100%) |
| | Hispanic | 1 (4%) | 0 | 1 (10%) | 0 |
| | Other | 9 (37%) | 6 (46%) | 4 (40%) | 0 |
| Stanford Cohort | | n = 24 | n = 12 | n = 7 | n = 5 |
| Sex | Female | 13 (54%) | 5 (42%) | 5 (71%) | 3 (40%) |
| | Male | 11 (46%) | 7 (58%) | 2 (29%) | 2 (60%) |
| Age | Mean (\pm SD) | 59.0 (\pm 16.1) | 57.0 (\pm 18.1) | 54.4 (\pm 12.1) | 70.0 (\pm 12.9) |
| | Range | 31 - 91 | 32 - 91 | 31 - 70 | 57 - 86 |
| Race | Asian | 7 (29%) | 3 (25%) | 2 (29%) | 2 (40%) |
| | Caucasian | 11 (46%) | 6 (50%) | 4 (57%) | 1 (20%) |
| | Hispanic | 2 (8%) | 2 (13%) | 0 | 0 |
| | Other | 4 (17%) | 1 (8%) | 1 (14%) | 2 (40%) |

Table S2. Cohort characteristics for UOP and STA cohort.

| Adjuvant therapy | None | RTx | CRTx |
|---------------------------------------|-------------|------------|-------------|
| All | | | |
| All cases (n = 24) | 13 | 7 | 4 |
| Higher vs. lower grade | | | |
| Lower grade (n = 12) | 8 | 3 | 1 |
| Higher grade (n = 12) | 5 | 4 | 3 |
| WHO Grade | | | |
| Grade 1 (n = 12) | 8 | 3 | 1 |
| Grade 2 (n = 7) | 4 | 1 | 2 |
| Grade 3 (n = 5) | 1 | 3 | 1 |
| Recurrence within three years | | | |
| Yes (n = 9) | 4 | 3 | 2 |
| No (n = 14) | 9 | 3 | 2 |
| Not documented (n = 1) | 0 | 1 | 0 |
| Cancer death within five years | | | |
| Yes (n = 7) | 2 | 3 | 2 |
| No (n = 17) | 11 | 4 | 2 |

Table S3. Adjuvant treatment and patient outcomes in the STA cohort.
RTx = radiotherapy, CRTx = chemoradiotherapy.